Evolution, 2023, **77(12)**, 2533–2546
https://doi.org/10.1093/evolut/qpad160
Advance access publication 6 September 2023
Original Article

OXFORD

The fitness landscape of a community of Darwin's finches

Marc-Olivier Beausoleil[1], Paola Lorena Carrión[1], Jeffrey Podos[2], Carlos Camacho[3], Julio Rabadán-González[4], Roxanne Richard[1], Kristen Lalla[5], Joost A.M. Raeymaekers[6], Sarah A. Knutie[7], Luis F. De León[8], Jaime A. Chaves[9,10], Dale H. Clayton[11], Jennifer A.H. Koop[12], Diana M.T. Sharpe[13], Kiyoko M. Gotanda[1,14,15,16], Sarah K. Huber[17], Rowan D.H. Barrett[1], Andrew P. Hendry[1]

[1]Redpath Museum and Department of Biology, McGill University, Montréal, Québec, Canada
[2]Department of Biology, University of Massachusetts Amherst, Amherst, MA, United States
[3]Department of Ecology and Evolution, Estación Biológica de Doñana—CSIC, Sevilla, Spain
[4]Observation.org Spain, Almensilla, Seville, Spain
[5]Department of Natural Resource Sciences, McGill University, Sainte-Anne-de-Bellevue, Québec, Canada
[6]Faculty of Biosciences and Aquaculture, Nord University, Bodø, Norway
[7]Department of Ecology and Evolutionary Biology, Institute for Systems Genomics, University of Connecticut, Storrs, CT, United States
[8]Department of Biology, University of Massachusetts Boston, Boston, MA, United States
[9]Department of Biology, San Francisco State University, San Francisco, CA, United States
[10]Colegio de Ciencias Biológicas y Ambientales, Universidad San Francisco de Quito, Quito, Ecuador
[11]School of Biological Sciences, University of Utah, Salt Lake City, UT, United States
[12]Department of Biological Sciences, Northern Illinois University, DeKalb, IL, United States
[13]Department of Organismic and Evolutionary Biology, Harvard University, Cambridge, MA, United States
[14]Department of Biological Sciences, Brock University, St. Catharines, Ontario, Canada
[15]Department of Zoology, University of Cambridge, United Kingdom
[16]Département de biologie, Université de Sherbrooke, Québec, Canada
[17]Virginia Institute of Marine Science, William and Mary, Gloucester Point, VA, United States

Corresponding authors: Redpath Museum, Department of Biology, McGill University, 859 Sherbrooke St. W., Montréal, Québec H3A 2K6, Canada. Email: marc-olivier.beausoleil@mail.mcgill.ca; andrew.hendry@mcgill.ca
R.D.H.B. and A.P.H. contributed equally to this work.

Abstract

Divergent natural selection should lead to adaptive radiation—that is, the rapid evolution of phenotypic and ecological diversity originating from a single clade. The drivers of adaptive radiation have often been conceptualized through the concept of "adaptive landscapes," yet formal empirical estimates of adaptive landscapes for natural adaptive radiations have proven elusive. Here, we use a 17-year dataset of Darwin's ground finches (*Geospiza* spp.) at an intensively studied site on Santa Cruz (Galápagos) to estimate individual apparent lifespan in relation to beak traits. We use these estimates to model a multi-species fitness landscape, which we also convert to a formal adaptive landscape. We then assess the correspondence between estimated fitness peaks and observed phenotypes for each of five phenotypic modes (*G. fuliginosa*, *G. fortis* [small and large morphotypes], *G. magnirostris*, and *G. scandens*). The fitness and adaptive landscapes show 5 and 4 peaks, respectively, and, as expected, the adaptive landscape was smoother than the fitness landscape. Each of the five phenotypic modes appeared reasonably close to the corresponding fitness peak, yet interesting deviations were also documented and examined. By estimating adaptive landscapes in an ongoing adaptive radiation, our study demonstrates their utility as a quantitative tool for exploring and predicting adaptive radiation.

Keywords: Darwin's finches, adaptive landscapes, speciation, adaptive radiation, Galápagos Santa Cruz, ecological theory,

Introduction

The concept of adaptive landscapes has been conceptually compelling yet empirically elusive. The phenotypic version of these landscapes (as opposed to their genetic counterpart developed by Wright [1932]) depicts multivariate relationships between mean population fitness and mean phenotype, which then—in conjunction with additive genetic (co) variances—can predict the progress and outcome of adaptive radiations (Arnold et al., 2001; Hendry, 2017; Lande, 1976; Schluter, 2000; Simpson, 1944). Adaptive landscapes are generally expected to be "rugged"—with multiple peaks of high fitness separated by valleys of lower fitness (Schluter, 2000). Adaptive radiation is often fueled by ecological speciation, which occurs when divergent natural selection splits an ancestral species occupying one fitness peak into new populations that bridge fitness valleys and occupy new fitness peaks (Hendry, 2017; Nosil, 2012; Schluter, 2000). Partly as a consequence of this adaptive divergence, reproductive isolation then evolves among the descendent populations (Schluter, 2000). This process then repeats to generate a larger adaptive

Received April 5, 2023; revisions received June 22, 2023; accepted August 31, 2023
Associate Editor: Catherine Wagner; Handling Editor: Tracey Chapman

radiation composed of multiple reproductively isolated species each occupying a different fitness peak on the adaptive landscape (Nosil, 2012; Schluter, 2000).

It has proven difficult to characterize adaptive landscapes in wild populations, and we therefore have a limited understanding of the fitness peaks and valleys expected to shape adaptive radiation (Fear & Price, 1998; Gavrilets, 2004; Svensson & Calsbeek, 2012a). In principle, data are required on individual fitnesses for the full range of phenotypes characterizing the existing species—as well as any phenotypic "gaps" between them that might not be occupied by existing phenotypes. The resulting individual "fitness landscape" then needs to be converted to a formal "adaptive landscape" by calculating mean fitness across an expected distribution of phenotypes for populations (conceptually) centered at every possible location on the individual fitness landscape (Arnold et al., 2001; Schluter, 2000). The conversion between these two landscape types is needed because theory has shown that the evolution of mean phenotypes should proceed in the direction of the steepest increase in the *population mean fitness*, with an attendant bias dictated by the structure of the genetic covariance matrix (Fear & Price, 1998; Lande, 1979). Therefore, to predict the dynamics of adaptive radiation, it is necessary to describe not just the individual fitness landscape but also the surface of mean phenotypes and mean fitness: that is, the adaptive landscape. Accomplishing these tasks is such a tall order that a formal adaptive landscape has never been estimated for an adaptive radiation in its natural environment.

Lacking formal estimates of adaptive landscapes, several proxies have been developed (Hendry, 2017; Schluter, 2000). For instance, estimates of phenotypic selection in natural populations can be used—with numerous assumptions—to infer the location of fitness peaks and curvature of the adaptive landscape in the vicinity of existing phenotypes (Beausoleil et al., 2019; Estes & Arnold, 2007; Smith, 1993). Furthermore, expected fitness for phenotypes in the gaps between existing populations can be inferred by generating "missing" phenotypes through simulated morphologies (McGhee, 2006; Raup, 1967; Tseng, 2013), phenotypic manipulations (Sinervo et al., 1992), hybridization (Arnegard et al., 2014; Martin & Wainwright, 2013), or reciprocal transplants (Nagy, 1997; Nagy & Rice, 1997). Finally, performance-based expectations can be used to translate resource distributions into expected fitness functions across the range of phenotypes (Schluter & Grant, 1984; Benkman, 2003; see Stayton, 2019 and Holzman et al., 2022 for performance surfaces). Studies using these proxies for adaptive landscapes have supported some expectations laid out in the ecological theory of adaptive radiation. In particular, the phenotypic distributions of at least some species pairs are centered on different fitness peaks and separated by fitness valleys that arise from different environments defined by resources, predators, parasites, or competitors (reviews: Hendry, 2017; Schluter, 2000).

Although studies using the above proxies have inferred rugged genotype or phenotype fitness landscapes (Martin & Gould, 2020; Pfaender et al., 2016; Schemske & Bradshaw, 1999), several uncertainties continue to surround the concept, interpretation, and application of adaptive landscapes, and even the individual fitness landscapes that underpin them. First, key aspects of many fitness landscape estimates might be unrealistic because they were (a) generated in controlled experimental settings (Arnegard et al., 2014; Benkman, 2003; Martin & Gould, 2020; Martin & Wainwright, 2013); (b) estimated at one location and then projected to other locations (Schluter & Grant, 1984); or (c) based on only one species with multiple morphotypes, such as Red Crossbills (*Loxia curvirostra*; Benkman, 1993, 2003) or Black-bellied Seedcrackers (*Pyrenestes ostrinus*; Smith, 1990; Smith & Girman, 2000). Second, fitness landscapes are rarely estimated over more than a single time frame (e.g., one season or one year) at any particular location, even though selection is expected to vary through time in accordance with changing conditions (Beausoleil et al., 2019; Schluter, 2000; Siepielski et al., 2009). As a result, we still have only a rudimentary understanding not only of adaptive landscapes but also their underlying individual fitness landscapes—especially for multiple species within natural adaptive radiations over multiple years (but see Martin & Gould, 2020). Thus, our main goal in the present study is to estimate the fitness landscape thought to underlie the adaptive landscape for Darwin's ground finch species (*Geospiza* spp.) at a single location over nearly two decades (2003–2020). We then use the estimated fitness landscape to consider theoretical expectations and previous empirical assertions regarding the topology of fitness and adaptive landscapes.

Study system

Darwin's finches started to radiate on the Galápagos about 1.5 million years ago (Lamichhaney et al., 2015, 2016; Petren et al., 2005); however, radiation of the ground finch (*Geospiza*) group was more rapid and recent, perhaps starting between 100,000 and 400,000 years ago (Lamichhaney et al., 2015). The primary phenotypic driver of this radiation at all phylogenetic levels is thought to be variation in beak (and body) size and shape (Bowman, 1961; Grant, 1999; Lack, 1947). In particular, beak dimensions are highly heritable (Boag, 1983), are influenced by large effect genes (Chaves et al., 2016; Lamichhaney et al., 2016), are linked to resource consumption (De León et al., 2014; Schluter & Grant, 1984), contribute to assortative mating (Huber et al., 2007; Podos, 2010; Ratcliffe & Grant, 1983), and show extensive variation linked to individual fitness (Beausoleil et al., 2019; Grant & Grant, 1995; Hendry et al., 2009). Other traits are surely also involved in the radiation, but work to date suggests that changes in beak dimensions have played a primary role.

Here, we focus on an intensively studied ground finch community at the relatively undisturbed location of El Garrapatero, Santa Cruz island, Galápagos. The four species of ground finch at this site—and at nearby sites on Santa Cruz—generally manifest five phenotypic modes (Beausoleil et al., 2019; Ford et al., 1973; Foster et al., 2008; Hendry et al., 2006; Lack, 1947; Supplementary Figure S1). First, the cactus finch (*Geospiza scandens*) has a long and pointy beak that it uses for consuming the nectar, pollen, and seeds of cactus plants in the genus *Opuntia* (Grant, 1999). Second, the small ground finch (*Geospiza fuliginosa*) has a small and blunt (i.e., not elongated like *G. scandens*) beak that it uses for cracking small seeds of a diversity of plant species (De León et al., 2014). Third, the large ground finch (*Geospiza magnirostris*) has a large and blunt beak that it often uses for cracking large and hard seeds of a few key plant species (Carvajal-Endara et al., 2019; De León et al., 2014). Fourth, the medium ground finch (*Geospiza fortis*) manifests two beak size modes (small and large "morphs") that fill out the distribution between *G.*

fuliginosa and *G. magnirostris* (Beausoleil et al., 2019; De León et al., 2014; Foster et al., 2008; Hendry et al., 2006). These two morphs appear to partition the middle of the seed size and hardness distribution along the same diet and performance axis that separates them from their smaller and larger congeners (De León et al., 2010, 2011). The evolutionary origin of these two morphs is uncertain, but hybridization with *G. magnirostris* is probably involved (Chaves et al., 2016).

Our intensive work on the ground finch community at this location affords a rare opportunity to estimate fitness landscapes in a natural system. Specifically, although five peaks are evident in the beak size and shape distribution, the presence of birds with intermediate beaks produces a continuum of phenotypes, allowing us to infer a fitness landscape across nearly the entire range of trait variation. Furthermore, our 17-year (2003–2020) mark-recapture dataset allows us to integrate viability selection and inferences about lifespans across a wide range of environmental conditions, from very wet El Niño years to very dry La Niña years (Beausoleil et al., 2019; Supplementary Figure S2).

Our goals

Using our long-term data set of the five phenotypic modes across four species of Darwin's ground finches at El Garrapatero, we examine (a) features of the fitness landscape, and (b) correspondence between those features and the phenotypic distribution.

Features of the fitness landscape

The basic dynamic underlying adaptive divergence is that different environments select for different combinations of trait values best suited for those environments (Darwin, 1859; Lack, 1947; Simpson, 1944). Hence, the fitness landscape for finch beak traits is expected to have peaks separated by valleys or surrounded by "moats" (Schluter, 2000). That is, the fitness landscape should not be flat, nor should it be a simple plane or saddle that lacks defined peaks. Furthermore, the fitness landscapes underlying adaptive *radiations* should be "rugged," with multiple fitness peaks at different combinations of trait values (Schluter, 2000). What remains uncertain, however, is just how many peaks are available to a given adaptive radiation (Hendry, 2017; Nosil, 2012; Schluter, 2000). The typical expectation might be that as many peaks exist as do species (more about this below), yet it is also possible for multiple species to evolve on a single fitness "ridge" (Schluter, 2000). We here test the classic expectation by modeling a fitness landscape across the entire range of data and species.

Correspondence between fitness and phenotypes

Adaptation is expected to drive the evolution of populations and species such that their phenotypes become localized near peaks on the fitness landscape (Arnold et al., 2001; Schluter, 2000; Schluter & Nychka, 1994). However, how many peaks are "occupied" by species (see the above expectation), and how close those species' phenotypes are to the peaks, is typically uncertain (Estes & Arnold, 2007; Hendry, 2017; Schluter, 2000). With regard to the second uncertainty, it has been variously argued that phenotypic distributions should closely match fitness landscapes (Estes & Arnold, 2007; Schluter, 2000) or that various constraints (e.g., gene flow, genetic correlations, environmental change) cause substantial maladaptation such that mean phenotypes will often be "far" from fitness peaks (reviews: Brady et al., 2019a, 2019b). We here address these uncertainties by estimating various measures of the distance between phenotypic modes and different peaks on the fitness landscape.

Our previous work on natural selection in this study system sets the stage for the present expanded effort. First, Hendry et al. (2009) showed that, in drought years (2004–2006), viability selection disfavored individuals between the two *G. fortis* beak size modes (i.e., they recorded disruptive selection between the modes). This viability selection also disfavored the largest and smallest individuals of that species, thus suggesting stabilizing selection around each beak size mode within this species. Second, Beausoleil et al. (2019) analyzed additional years of data and showed that disruptive selection between the *G. fortis* beak size modes varied through time in a manner that was partly predictable based on the amount of rainfall in the preceding year. Both of those studies took a single-species approach to the fitness landscape, thus limiting inferences about adaptive radiation of the ground finch community as a whole. Here, we use an even longer time series and a multi-species approach to estimate the fitness landscape and thus inform our understanding of the process of adaptive radiation.

Methods

Long-term data

From 2003 to 2020, we used mist nets to capture ground finches at El Garrapatero (Santa Cruz, Galápagos, Ecuador; 0°41′22.9″ S, 90°13′19.7″ W; Supplementary Figure S3A). The specific net locations were chosen for accessibility; that is, they were situated in relatively open areas within a larger 0.43 km^2 study site (Supplementary Figure S3B). Sampling took place in the typical finch breeding season (January–April), with year-to-year variation in the dates and duration of sampling (Supplementary Figure S4; Supplementary Table SI) that reflected logistical constraints. In most years, effort was directed at ensuring that all ground finch species were a part of the study; however, in the earliest years (2003–2009), effort was primarily focused on *G. fortis*. Hence, the relative numbers of captured birds of the different species do not necessarily reflect variation in natural patterns of relative abundance.

Captured finches were fitted with individually numbered aluminum or Monel metal leg bands. Each bird was then measured for beak length, depth, and width (the classic measurements used to infer variation in this radiation; Grant, 1999)—always with calipers having a precision of 0.01 mm (further details appear in De León et al., 2012). In many cases, each measurement was taken three times, and the median value was used for subsequent analyses—thus reducing measurement error. The mean repeatability (intra-class correlation coefficient) of beak trait measurements (length, depth, and width) based on the same birds captured at different times was 0.92. Repeatability was calculated from birds with three measurements by the same observer using a random effect of bird band number in the rptR package (Stoffel & Nakagawa & Schielzeth, 2017; version 0.9.22). Only individuals for which we obtained all three beak measurements (length, depth, and width) were retained for subsequent analyses (n = 3,428; Supplementary Table SII).

The four recognized species (*G. fuliginosa*, *G. fortis*, *G. magnirostris*, and *G. scandens*) were identified based on

classic visual assessment (Grant, 1999), which we have confirmed to be very reliable (Foster et al., 2008). To further assign birds of the medium ground finch (*G. fortis*) to one of the two "morphs" or "modes" (Hendry et al., 2006), we used an expectation–maximization algorithm model from the mixtools R package based on the first principal component (beak size) calculated from the three beak traits of all species (Benaglia et al., 2009; version 1.2.0; see Beausoleil et al., 2019). Note, however, that the phenotypic distribution is continuous, and so birds in the valley between the two modes could not be reliably assigned to one or the other "morph." Furthermore, although the distributions for small *G. fortis* versus *G. fuliginosa* are relatively discrete (i.e., a small gap exists between them; Supplementary Figure S1; Supplementary Figure S5), the distribution for large *G. fortis* grades continuously into *G. magnirostris*, again indicating that intermediate birds could not be reliably assigned to one or the other species. However, these ambiguities do not impact our analyses as we are considering the entire phenotypic distribution across all species.

Converting capture history into a fitness metric

We estimated the individual fitness for each bird from its capture history. One approach here could have been a year-by-year survival estimate—as indeed we have employed in previous work that focused on the species (*G. fortis*) over a subset of the years (2003–2011) that had by far the largest sample sizes (Beausoleil et al., 2019). Here, however, we needed the best possible survival-based fitness surrogate across all species, some of which had low sample sizes in any given year. Thus, to achieve our community-wide fitness landscape, we here instead used the "apparent lifespan" of a bird as the best obtainable surrogate for fitness; and, indeed, lifespan is known to be a major determinant of fitness variation in *Geospiza* (Grant & Grant, 2000, 2011). We estimated apparent lifespan as the last year a bird was captured minus the first year that bird was captured. Only captures of adult birds were included; 28 individuals were first caught as juveniles, but later became adults and were then analyzed as adults. This apparent lifespan estimate is thus a minimum (when rounded to the number of years) of the true lifespan of a bird; that is, most birds would have been alive for at least one year before their first capture and would continue living for an unknown period of time after their last capture. Note that our fitness surrogate thus does not discriminate between mortality and emigration but, fortunately, both processes are functionally equivalent at the level of the population: that is, both represent the loss of individuals from the local area. We focused our fitness landscape estimates on two traits: beak length and beak depth. The reasons were twofold. First, we could retain the original trait values in the analysis, which allows representation of the fitness landscape using raw trait values that also correspond to published estimates of additive genetic (co) variances (See section "Prospective Selection" below; Boag, 1983). Second, these two traits have been identified as key targets of selection in finches (Boag & Grant, 1984; Price et al., 1984; Schluter, 2000). Beak width was not analyzed because the Pearson correlation between beak depth and beak width was very high ($r = .97$, $p < .001$). By contrast, the correlation between beak length and depth was much lower (Pearson correlation $r = .74$, $p < .01$)—and therefore both traits (and their combination) were informative.

We note, however, that many papers analyze all three traits based on their re-orientation into two primary principal component analysis (PCA) axes. Indeed, many of our previous papers on this system have taken that approach (Beausoleil et al., 2019; Chaves et al., 2016; Hendry et al., 2006, 2009). Therefore, as a supplement, we also estimated the fitness landscape for the two first principal components describing beak size and shape (respectively) based on the combination of beak length, depth, and width. We used the vegan package (Oksanen et al., 2022; version 2.6-4) to calculate the principal components on the three beak dimensions across all birds included in the analysis. The thin plate spline generalized additive models (GAM) generated the fitness landscape ($f(z)$), with apparent lifespan against beak size (PC1) and beak shape (PC2) as previously described in the main text except for the thin plate regression spline, which had 4 and 19 dimensions for the bases (k) of the smooth function and the interaction smooth function, respectively.

Fitness landscape model

We decided to estimate a single fitness landscape that integrates information from all birds across all years—as opposed to year-specific or climate-specific surfaces. The reasons were threefold. First, evolutionary differences on the relevant scale of inference (i.e., the distribution of beak traits in a community of finches) is a function of the long-term "average" surface, as opposed to year-specific surfaces. Second, by leveraging all of our data into a single fitness landscape estimate, we hoped to obtain a comprehensive long-term "best" estimate of the surface—as opposed to less precise year-specific estimates. Finally, our fitness measure is an estimate of lifespan, which necessarily spans multiple years for many birds, and so cannot be parsed into subsets of those years. For year-specific estimates based on annual survival for part of this fitness landscape (*G. fortis* for the years 2004–2011), we refer the reader to Beausoleil et al. (2019).

To generate the single integrated fitness landscape ($f(z)$), we plotted apparent lifespan (W, expected fitness, estimated as above) against individual beak length and beak depth (z). We started with a model-free estimate by calculating the natural-logarithm of mean fitness by mean phenotype in phenotypic "windows" (bins) of 0.14 mm (Figure 1A). Binning of individual fitness values smooths the landscape from the raw data and makes it possible to diagnose some key features. Second, we used the individual fitness estimates and beak traits in thin plate spline GAM with a Poisson response variable, applying the smooth function s as an interaction between traits and the *gam* function in the mgcv package (version 1.8-39; R Core Team, 2023; Wood, 2003; Wood et al., 2013, 2016). Note that GAMs are a modern flexible approach to studying complex fitness landscapes (Martin & Gould, 2020; Patton et al., 2022) that have largely replaced the formerly favored projection pursuit regressions (Schluter & Nychka, 1994; Supplementary Figure S6), with the latter technique also being more focused on dimension reduction which was not necessary here given our focus on only two traits. The curvature of the function was estimated using smoothing parameters determined by restricted maximum likelihood, with an extra term to allow a penalty of 0 (removing this option did not change the results; Supplementary Figure S7) in a thin plate regression spline with 4 and 27 dimensions for the bases (k) of the smooth function and the interaction smooth function, respectively.

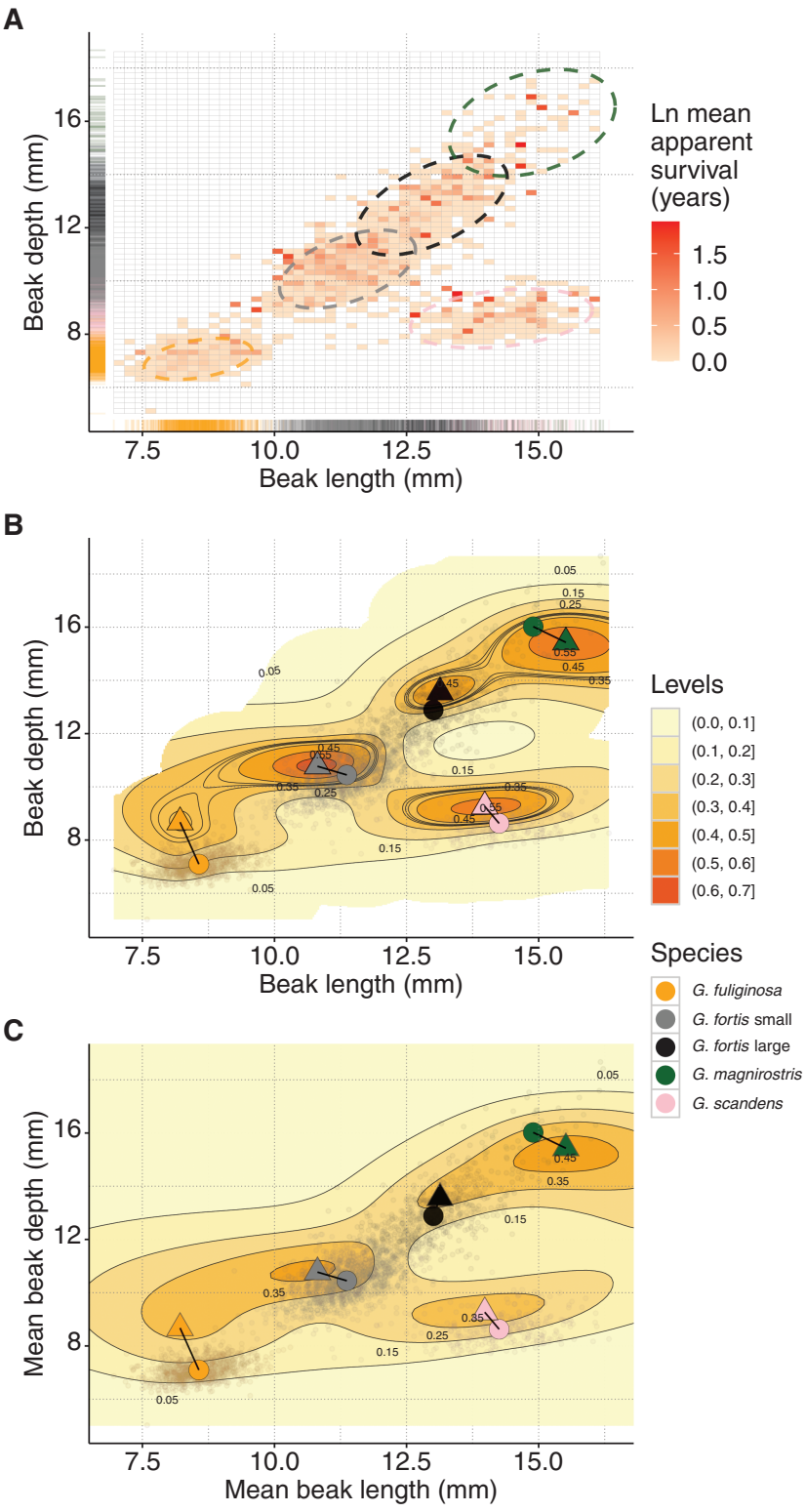

Figure 1. Fitness and adaptive landscape of *Geospiza* spp. at El Garrapatero (Santa Cruz Island). (A) fitness Ln-transformed mean for bins of phenotypes without model by increments of 0.14 mm. The ellipses are 95% multivariate t-distributions based on the individual beak phenotypes of each species. (B) Individual-based fitness landscape from the spline model. Note that there are more contour lines compared to the legend to show the peaks more clearly. (C) the adaptive landscape is obtained by "moving" a simulated population for each phenotypic mean and mean predicted fitness. The fitness landscape spline model predicted the fitness values of the simulated population to generate the adaptive landscape (Schluter, 2000). The color scale is scaled to be comparable between the figures. The triangles are the local fitness peak maximum and the large points are the population phenotypic means for the various modes of ground finches (smaller transparent points are the data for each bird). Distances between fitness peaks (triangles) and population means (larger points) were calculated using Euclidean distances. The standard error of the fitness landscape can be found in Supplementary Figure S9.

To then examine the correspondence between the fitness landscape peaks and the five phenotypic modes, we developed a function to locate the fitness peaks, which then could be compared to the finch modes as mean trait values. Specifically, we calculated phenotypic Euclidean distances between the fitness peak and the phenotypic mean of each mode, as well as the angle of each Euclidean distance vector counterclockwise from the positive side of the x-axis, representing beak length. These Euclidean distances represent the shortest distances in two-dimensional phenotypic space between the fitness peaks and the phenotypic means.

Adaptive landscape estimate

Adaptive landscape estimation requires the conversion of an individual fitness landscape (as above) to a landscape of mean fitnesses $(\bar{W})$ for a population with a given phenotypic mean $(\bar{\mathbf{z}})$ and variance (Fear & Price, 1998; Schluter, 2000). To make this conversion, we simulated—across the entire phenotypic range—a hypothetical population with a bivariate normal distribution with a mean (standard deviation) beak length and beak depth across species of 12.42 mm (0.67 mm) and 11.02 mm (0.69 mm), respectively and a correlation of r = .39 (mean coefficients of variation [standard deviation divided by mean] of 5.4% and 6.2% for beak length and beak depth). We used *rnorm_multi* function from the faux package (DeBruine, 2021; version 1.2.0; note that when we used the phenotypic distribution of the small morphotype of *G. fortis*, it did not significantly change the adaptive landscape compared to the one with simulated data, see Supplementary Figure S8). We generated a 90 × 90 point-grid (the distance between each point of the grid was 0.13 mm (beak length) and 0.17 mm (beak depth)) covering the phenotypic space of each trait. We then centered the hypothetical population at the mean of the two phenotypic distributions $(\bar{\mathbf{z}})$ on each point on the grid (Schluter, 2000). Finally, we calculated the mean fitness values $(\bar{W})$ based on their expected fitness $f(\mathbf{z})$ from the fitness landscape (spline model) on the transformed (link) scale for each point on the grid (see Animation S1).

Prospective selection

An evolutionarily informed estimate of the distance between population phenotypes and adaptive peaks can be calculated as the amount of selection that would be required to complete an adaptive shift to that peak. We performed this calculation using the multivariate equation of evolutionary phenotypic change, where the vector of changes in mean trait values $(\Delta\ \bar{\mathbf{z}})$ is a product of the additive genetic variance-covariance matrix $(\mathbf{G})$ for those traits and the vector of selection gradients $(\boldsymbol{\beta})$ acting on those traits. That is, $\Delta\ \bar{\mathbf{z}} = \mathbf{G}\boldsymbol{\beta}$ (Lande, 1979; Schluter, 1984, 2000). Rearranging this equation for species in an existing adaptive radiation gives what Schluter (1984) called "retrospective selection" $\left(\Delta\ \boldsymbol{\beta} = \mathbf{G}^{-1}\bar{\mathbf{z}}_b - \mathbf{G}^{-1}\bar{\mathbf{z}}_a\right)$, where the subscripts "b" and "a" represent the phenotypic values of different populations. Using this approach, Schluter (1984, 2000) estimated the amount of selection that would have been required in the past (hence "retrospective") to generate the phenotypic differences that currently exist among species in the finch radiation.

In our case, we used the approach to estimate the amount of selection that would be required for each phenotypic mode to reach its nearest adaptive peak (hence "prospective" which we note as $\boldsymbol{\beta}_p$). In our cases, $\Delta\ \bar{\mathbf{z}}$ was the distance between the bivariate trait mean of each of the five phenotypic modes and the nearest bivariate phenotypic optimum on the individual fitness landscape. For **G**, we used the genetic variances and covariances for *G. fortis* estimated in Boag (1983)—the same values used by Schluter (1984, 2000). The resulting **G**-transformed beak trait differences in Euclidean space represent the net selection gradients that would be needed to bridge the distances between the current phenotypic means and their nearest fitness peaks on the individual fitness landscape. Note that this approach is simply a way of providing a genetic context for phenotypic distances and is not intended to estimate the actual selection that would occur during such evolution. In particular, the approach requires a number of restrictive assumptions, including constancy of the **G** matrix, that all relevant correlated traits are included, and that the difference in population means is genetically based. The code for the analyses is available at the Borealis dataverse (Beausoleil et al., 2023) and on GitHub https://github.com/beausoleilmo/adaptive.landscapes.finches.

Results

Of the 3,428 individuals analyzed in our study, 3,038 (88.6%) were captured only once, whereas 390 birds were captured across multiple years (fitness > 0). Minimum lifespans of these birds ranged from 1 to 12 years (Supplementary Table SII). The species with the highest proportion of recaptured individuals in the dataset was of the small morphotype of *G. fortis* (40.4%), whereas the lowest proportion of individuals were *G. magnirostris* (1.5%; Supplementary Table SII).

The GAM-estimated individual-based fitness landscape is shown in Figure 1B, and its standard error is shown in Supplementary Figure S9. To select the appropriate topology for this landscape, we designed a model including a smoothing term for each trait and an interaction between the two traits. We started with the smallest dimension parameter (k, an arbitrary number chosen by the user to reflect the non-linearity in the data; it defines the number of basis functions used to calculate the smooth line in GAMs) for each smoothed function of the traits and incrementally increased this parameter until the model showed the simplest peaked landscape. We compared this model to a model without the interaction and to another model with only the intercept. The significant smoothing term in the model was the interaction between beak length and beak depth (p<<.01; 20.27 effective degrees of freedom; Supplementary Table SIII). That is, the smoothed model was much better supported than a similar model including only the intercept (the difference in AIC between the intercept model without smoothing and the smoothed model was ΔAIC = 192.04, where a lower AIC (for the smoothed model) indicates a better-fit model; likelihood ratio tests with p<<.01, difference in deviance = 238.65; Supplementary Table SIV). Therefore, the rest of the analyses used the model with the main effects and the interaction between the two beak traits.

Features of the fitness landscape

The individual fitness landscape estimated for beak length and depth revealed five peaks, each separated from adjacent fitness peaks by fitness valleys (Figure 1B). In a number of cases, those valleys were deep. Consider, for instance, the fitness peak nearest to *G. scandens*. In a straight line (in Euclidean phenotypic space) from that peak to each of

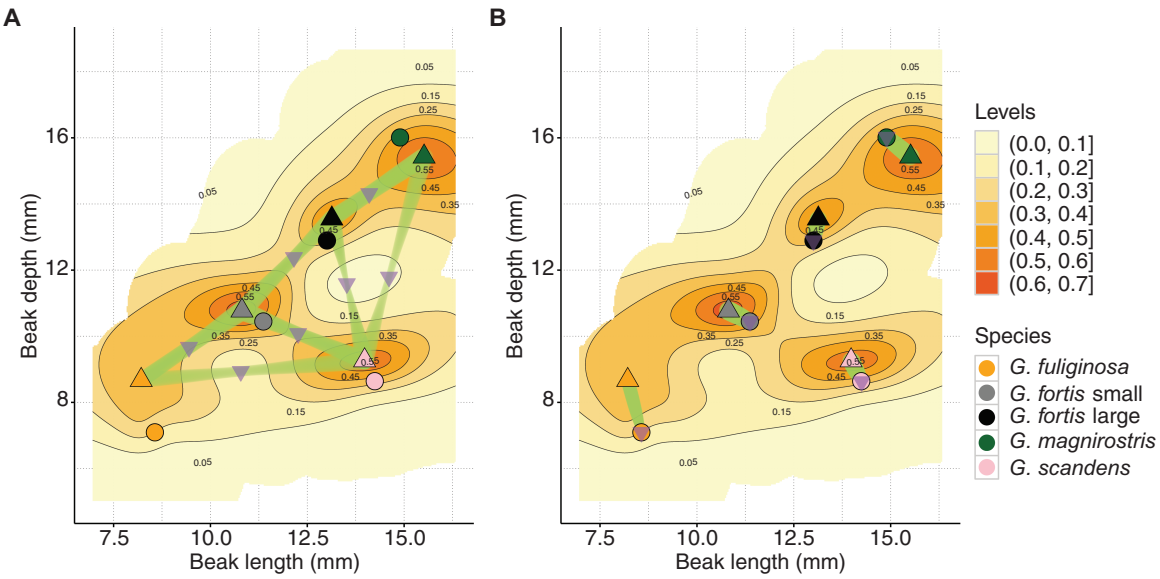

Figure 2. Fitness landscape with lines (in green) connecting the fitness peaks of (panel A) all *Geospiza* spp. and (panel B) from fitness peak-mean phenotypes of each species. The down-pointing purple triangle represents the minimum on that line. Note that the minimum fitness in panel B is at the phenotypic mean for each species (the triangle overlaps the point for a population phenotypic mean). Values in panels A and B are found in Supplementary Tables SV and SVII, respectively.

the other peaks (Figure 2A; Supplementary Table SV), fitness declined by 84.08% (minimum fitness toward the peak nearest *G. magnirostris* relative to the maximum fitness of *G. scandens*), 86.58% (toward the peak nearest the large morph of *G. fortis*), 47.74% (toward the peak nearest the small morph of *G. fortis*), and 71.13% (toward the peak nearest *G. fuliginosa*). The fitness valley was also especially deep between the two peaks nearest the *G. fortis* beak size morphs: wherein fitness declined by 60.64% moving from small *G. fortis* toward large *G. fortis*, and by 48.48% moving in the other direction. By contrast, the fitness valley was shallow—indeed, almost absent (17.04%)—between the peak nearest *G. fuliginosa* and the peak nearest the small morph of *G. fortis*.

The basic "rugged" property of this individual fitness landscape was conserved in an alternative representation based on principal components of beak "size" and "shape" (Supplementary Figure S10). In this supplementary analysis, PC1 can be interpreted as beak size (loadings in absolute values for beak length = 7.3, depth = 9.0, width = 6.9 and variance explained by the first axis being 88.3%), with greater values indicating larger beaks; and PC2 can be interpreted as beak shape (loadings in absolute values for beak length = 4.0, depth = 2.2, width = 1.4 and variance explained being 10.9%), with greater values indicating pointier beaks. Using these PCA scores, a fitness landscape with three major peaks was apparent (Supplementary Figure S10). Finally, when converting the focal fitness landscape for beak length and depth (based on individual phenotypes and fitnesses: Figure 1B) to an adaptive landscape (based on simulated population mean phenotypes and predicted fitnesses), many of the same peaks remained evident, although relative differences between peak heights and valley depths were much reduced—as expected from such conversions (Schluter, 2000). In short, all analyses support the expectation that fitness landscapes—and the adaptive landscapes they underpin—are characterized by multiple fitness peaks separated by fitness valleys of varying depth.

Correspondence between fitness and phenotypes

Mean trait values for the five phenotypic modes (i.e., the four species in which *G. fortis* separates in two distinct morphs) were situated reasonably close to their corresponding fitness peaks. For instance, the mean Euclidean distance between bivariate (beak length and depth) means (for the five modes) and their nearest peaks on the fitness landscape was 0.90 mm (range 0.64–1.62 mm; Figure 1; Table 1). By comparison, Euclidean distances among the various species phenotypic means averaged 5.69 mm (n = 10, range 2.94–10.94 mm; Supplementary Table SVI). Thus, the *shortest* distances among phenotypic modes exceeded the *largest* distances between each mode and their nearest fitness peaks.

Analyses of "prospective selection" ($\boldsymbol{\beta}_p$) that adjust phenotypic distances for the genetic (co)variances of traits yielded similar—but further nuanced—conclusions (Figure 3). For instance, $\boldsymbol{\beta}_p$ values for the distance between the five modes and their nearest fitness peaks averaged 1.59 (range 0.50–3.50; Table 1). By contrast, $\boldsymbol{\beta}_p$ values for the distance between means of the five modes averaged 3.27 (range 0.37–7.47; Supplementary Table SVI). In summary, each phenotypic mode was closer to its nearest peak than it was to the other phenotypic modes, but the differences in this comparison were diminished as we accounted for genetic correlations (Figure 3). We also found that the phenotypic modes were at a lower fitness on the fitness landscape compared to the closest peak (Figure 1; Supplementary Table SVII).

Although fitness estimates required use of the entire data set across all years (see Methods), phenotypic means could be estimated for each year, thus allowing us to consider whether the above inferences about phenotype-to-fitness correspondence showed noticeable temporal variation. We find that trait mean values for each of the five modes were reasonably similar across years—such that year-specific estimates were always oriented (in phenotypic space) in a similar direction and to a similar distance from the nearest fitness peak (Figure 4). Variation across years was highest for *G. magnirostris*, presumably due—at least in part—to its small sample size.

Table 1. Euclidean distances of population mean to the position of the peaks on the fitness landscape.

Species	Beak length (mm) [SD; CV]	Beak depth (mm) [SD; CV]	Peak position beak length (mm)	Peak position beak depth (mm)	Δlength; Δdepth coordinate (mm)[a]	Euclidean distance phenotypic mean-fitness peak (mm)	Euclidean distance phenotypic mean-fitness peak (scaled traits, sd units)	Angle of vector (°)[b]	Euclidean distance G-trans. phenotypic mean-G-trans.fitness peak	$\Delta\beta_p$[c] [G-beak length, G-beak depth]
G. fuliginosa	8.57 [0.49; 5.69]	7.10 [0.38; 5.29]	8.21	8.67	0.51; 2.08	1.62	4.26	102.70	3.50	[−2.77, 2.14]
G. fortis small	11.37 [0.60; 5.27]	10.45 [0.68; 6.53]	10.81	10.77	0.55; 0.37	0.64	1.04	149.71	1.36	[−1.11, 0.78]
G. fortis large	13.01 [0.67; 5.12]	12.89 [0.85; 6.63]	13.13	13.56	0.13; 0.67	0.68	0.81	76.33	0.50	[−0.38, 0.33]
G. magnirostris	14.90 [0.71; 4.76]	16.02 [0.93; 5.81]	15.52	15.43	0.65; 0.64	0.85	1.08	316.27	1.28	[1.04, −0.74]
G. scandens	14.25 [0.86; 6.01]	8.63 [0.54; 6.26]	13.98	9.27	0.27; 0.64	0.69	1.22	103.11	1.32	[−1.05, 0.80]
Mean						0.90	1.68	152.22	1.59	

Note. CV = coefficient of variation; *SD* = standard deviation
[a]Difference (Δ) in phenotypic space between the fitness peak and the population mean
[b]The angle is taken counterclockwise from the positive side of the x-axis, so that a 90° angle is pointing straight up in the y-axis.
[c]Distance $\Delta\ \boldsymbol{\beta} = \boldsymbol{G}^{-1}\bar{\boldsymbol{z}}_b - \boldsymbol{G}^{-1}\bar{\boldsymbol{z}}_a$ between the fitness peak and the population mean phenotypic traits (see Figure 1 panel B). The values represent the *G*-transformed beak traits (length and depth respectively.).

Discussion

Features of the fitness landscape

As expected from the ecological theory of adaptive radiation (Nosil, 2012; Schluter, 2000), the individual fitness landscape that we estimated for a community of ground finches showed a number of distinct peaks separated by fitness valleys. Depending on how the traits were represented, the number of estimated peaks varied from five (beak length vs. beak depth; Figure 1) to three (PC1 vs. PC2; Supplementary Figure S10). For the rest of this discussion, we focus on the five-peaked landscape because selection presumably acts more directly on the original traits (beak length and depth) than on statistically generated linear combinations of traits (PCs). However, we acknowledge that some of the more detailed inferences that follow are sensitive to the ways in which traits are represented. The general inferences, however, are robust to such variation. When reading the following, bear in mind that the inferences we present do not depend on which modes are considered to be separate "species" (we use the traditional designations), nor the specific manner in which those modes originated (e.g., via fission from a single ancestral source or fusion via hybridization between ancestral sources).

We also converted the above fitness landscape estimated for individual traits and fitnesses to an adaptive landscape for mean traits and fitnesses (Figure 1). Again, as expected from theory (Arnold et al., 2001; Schluter, 2000), the adaptive landscape was smoother than its underlying fitness landscape. The reason is that adaptive landscapes average individual fitnesses across a range of phenotypes—and so, relative to the fitness landscape, the peaks sink (because they include lower fitness values from either side of the peak) and the valleys rise (because they include higher fitness values from either side of the valley). This smoothing of the adaptive landscape tends to obscure some features of the fitness landscape, and is perhaps why previous analyses of adaptive radiations in vertebrates have not converted fitness landscapes to adaptive landscapes (Benkman, 1993; Smith, 1993; but see Schluter, 2000) or have instead generated resource-based adaptive landscapes (Schluter, 1984). In our case, the conversion of the individual fitness landscape to the adaptive landscape eliminated the valley between the large morph of *G. fortis* and *G. magnirostris* (more about this later) but retained the rest of the topology. Thus, our analysis shows that most key features of the fitness landscape are retained in the adaptive landscape, providing support for the empirical quantification of a function (the phenotypic adaptive landscape) that has thus far been mostly theoretical, heuristic, or aspirational for field studies of adaptive radiations (Arnold et al., 2001; Hendry, 2017; Schluter, 2000).

Correspondence of fitness and phenotypes

We found that phenotypic modes of the *Geospiza* are close to, but not directly on, their respective fitness peaks (Figure 1). The first part of this conclusion (i.e., "close to") supports the basic premise of the ecological theory of adaptive radiation that different resources (here different seed types) generate multiple phenotypic fitness peaks that promote diversification into different species (Arnold et al., 2001; Grant, 1999; Hendry, 2017; Nosil, 2012; Schluter, 1984; 2000). The second part of the conclusion (i.e., "not directly on") also is not unexpected (Brady et al., 2019a, 2019b), and affords an opportunity to discuss the reasons why adaptation (and adaptive

radiation) might be constrained in various ways. Some such constraints can be considered with our current analysis and by reference to previous studies within our study system.

First, introgression among species can constrain divergence from reaching the species' respective optima and, indeed, interbreeding and introgression are known to occur between *G. fortis* and each of the other *Geospiza* species as well as between the two *G. fortis* morphs (De León et al., 2010; Grant, 1993, 1999; Grant & Grant, 1992; 2021; Lamichhaney et al., 2015). This potential constraint predicts that species means will be displaced from fitness optima in the direction of the species from which introgression occurs. Such a pattern was not evident in our data for *G. fuliginosa*, *G. scandens*, or *G. magnirostris* (Figure 1B). By contrast, phenotypic modes for the *G. fortis* morphs did deviate from their fitness peaks in the direction of groups with which they hybridize (the large morph of *G. fortis* toward the small morph of *G. fortis*, and the small morph of *G. fortis* toward *G. scandens*)—but these deviations were among the smallest observed (Figure 1B). Introgression, therefore, seems unlikely to explain why the phenotypic modes were displaced to one side of their fitness peaks. Indeed, an increasing body of work argues that introgression is a creative rather than constraining force in adaptive radiation in general (Grant & Grant, 2019) and in Darwin's finches specifically (Lamichhaney et al., 2015).

Second, as with introgression (above), gene flow across populations within species can bias adaptation away from local optima (Bolnick & Nosil, 2007; Garant et al., 2007; Hendry & Taylor, 2004). Indeed, we expect considerable immigration and emigration for our "open" study site. (Note that emigration and mortality are functionally equivalent at the level of a population and so both are relevant to selection at that level.) Supporting this point, previous analyses have shown high levels of gene flow and connectivity across the island of Santa Cruz, at least for *G. fortis* (De León et al., 2010; Galligan et al., 2012; Petren et al., 2005). It seems unlikely, however, that the movement of birds across sites could be a primary driver of the deviations we observed between phenotypic modes and fitness peaks. In particular, the deviations we observed were not generally in the direction of another known population of each species (Carrión et al., 2022; Foster et al., 2008; Kleindorfer et al., 2006; See Supplementary Material and Supplementary Figure S11).

Third, genetic constraints can cause trait means to deviate from adaptive optima (Arnold et al., 2001; Svensson & Calsbeek, 2012a). For instance, ground finches generally show a positive genetic correlation between beak length and depth (Boag, 1983; Grant & Grant, 1994; Price et al., 1984), which could constrain evolution along orthogonal axes. We do not favor this possibility as an explanation for the deviations we observed between phenotypic modes and their estimated fitness optima. Consider our analysis of "prospective selection" (Figure 3), which scales trait differences by genetic correlations. In particular, when ignoring such correlations (i.e., Euclidean distances), the phenotypic distance between each phenotypic mode and the nearest optima (peak) was much smaller than phenotypic distances across modes. However, when including such correlations (i.e., estimates of "prospective selection"), the same type of comparison yielded a much smaller contrast. In other words, accounting for genetic correlations "shrinks" the distance among different phenotypic modes more than it shrinks the distance between each mode and its nearest fitness peak. This result suggests that diversification across the species was not strongly constrained by genetic (co)variances, except perhaps for *G. scandens*, which lies off the main axis of variation in having evolved long but shallow beaks (Grant, 1999); and yet *G. scandens* did, in fact, evolve. As such, it seems unlikely that genetic (co)variances constrain each of the species from reaching their respective fitness peaks.

Although each of the above constraints could contribute to the observed offsets between phenotypic modes and fitness peaks, none are likely an important causal factor. Instead, we suggest that the primary cause of observed deviations from fitness peaks is merely methodological. This suggestion comes from our observation that all displacements of mean phenotypes from fitness peaks in our analyses always fell in the same direction, an outcome that implies some sort of methodological bias (Figure 4). One possible bias is that adaptive radiation can be strongly influenced by rare events (De León et al., 2012; Grant & Grant, 2014), in which case fitness peaks estimated in some years might not reflect the fitness peaks that drove adaptive radiation in the first place. However, our dataset was long term (17 years) and integrated across very diverse ecological conditions (Supplementary Figure S2). Another possibility is that our fitness surrogate was biased in capturing only one of several key fitness components. For instance, we only used longevity, whereas fitness is also determined by reproductive success, which perhaps favors different trait values. It would take an entirely new and different set of data to address this possibility. Beyond this possible bias, some imprecision is also present in our estimates, owing principally to low sample sizes (especially for *G. magnirostris*) and low recapture rates (see Supplementary Material; Supplementary Figures S4 and S9). Resulting imprecision adds noise to our estimates of the fitness landscape, such that the true landscape might be much more refined than the one our data captures.

Future research and prospectus

The structure of fitness and adaptive landscapes depends on features of the environment, such as local resources and competition (Schluter, 2000) that vary dramatically across space. Hence, it would be informative, using similar techniques to those applied here, to construct fitness and adaptive landscapes for finch communities on other islands. Daphne Major is an obvious candidate as previous work has estimated lifetime fitness for finches at that site, which differs dramatically in environment and phenotype from our study site (Carrión et al., 2022; Grant & Grant, 2002, 2011, 2014). Another informative situation would be the community of ground finches at Academy Bay, Santa Cruz, where human influences have been inferred to strongly alter resources, selection, and adaptation (De León et al., 2011, 2018; Hendry et al., 2006). These formal landscapes then also could be compared to the resource-based landscape presented by Schluter (1984). Similar analyses could be applied to data for other adaptive radiations of birds and other organisms. A major limiting factor is likely to be the large effort and time required to do so with any degree of confidence, at least in the case of long-lived organisms such as finches.

Environmental features shaping adaptive radiation can also vary through time (Merrell, 1994); such effects could be examined by considering temporal variation in landscape estimates. Such an analysis was not possible in our case because our fitness surrogate (lifespan) required integration across the entire data set. However, our previous analysis of annual survival in *G. fortis* (the species with the largest sample size and

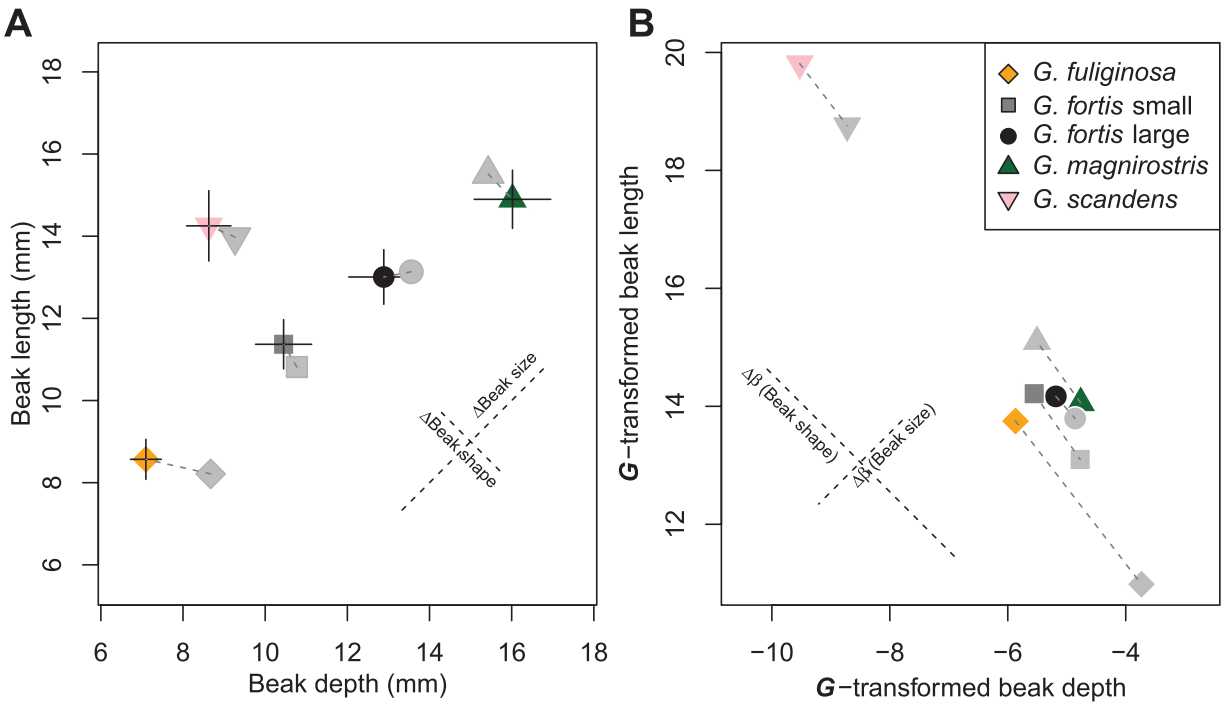

Figure 3. Prospective selection assuming finch populations would evolve toward their fitness landscape peaks. In panel A, colored points represent species means from our data, the points in gray with the corresponding shape for each species, are the positions of the fitness landscape peaks (Figure 1B). The vertical and horizontal bars are one standard deviation for the phenotypic traits. In panel B, the ***G***-transformed beak phenotypes (calculated via the genetic variance-covariance matrix (***G***-matrix) from a population of *G. fortis*, Boag, 1983) gives an idea of how much selection is required to make a population evolve in a certain direction. The distance between two points represents the net selection gradient required to move from one point to the other. In both panels, the dashed lines approximately represent the axes of beak size and shape for the raw traits.

best recapture rates) over 9 years at this site revealed notable associations between selection and environmental conditions (Beausoleil et al., 2019). Such variation is likely common given evidence not only of temporal environmental fluctuations, but also of temporal variation in selection coefficients acting on phenotypic traits (Siepielski et al., 2009, 2017). Accordingly, a goal for future work could be to compare, in natural populations, long-term estimates of adaptive landscapes to patterns of temporal variation in key environmental factors.

The ultimate promise of adaptive landscapes, as an analytic tool, is to link genetic architecture to selection and adaptive radiation (Arnold et al., 2001; Hendry, 2017; Schluter, 2000). Making these connections should, in theory, allow insight into the genetic constraints or opportunities that impede or facilitate the occupation of adaptive landscape peaks, shifts between them, and—thus—speciation and diversification (Patton et al., 2022; and reference therein). At present, however, estimates of the ***G*** matrix are extremely limited in the traits examined, the environments in which they are quantified, and the number of species in either case. Future ***G*** matrix estimations for species in adaptive radiations in their natural environments will be greatly facilitated through recent applications of genomic data to relatedness estimates, as used in "animal model" estimates (Kruuk, 2004; Wilson et al., 2010).

Is the "landscape concept" still useful today? It has been argued by a number of authors that the concept of the adaptive landscape has so many assumptions as to be unhelpful at best and misleading at worst (Kaplan, 2008; Pigliucci, 2008). Yet, at the same time, other authors have argued that the adaptive landscape concept remains a useful tool in a variety of fields, including population genetics, evolutionary ecology, conservation biology, and speciation (Gavrilets, 2004; Svensson & Calsbeek, 2012b). It is our view that adaptive landscapes are useful and informative, even if we still hold a poor understanding of many of their features such as their spatio-temporal dynamics, their sensitivity to assumptions (e.g., multivariate normality), their modification by density and frequency dependence, and many other subtle and not-so-subtle nuances (Svensson & Calsbeek, 2012a). Perhaps most daunting thus far, however, has been the inability of practicing biologists to actually generate empirically based adaptive landscapes for natural adaptive radiations.

Our analysis addresses this last criticism (of practicality) by showing that multi-species fitness landscapes can be used not just as a metaphorical concept but also as a quantitative tool for exploring the factors contributing to adaptive radiation. Our adaptive landscape for beak traits of *Geospiza* spp. unveiled the expected number of fitness peaks, with the phenotypes of four species (and two intra-specific "morphs") near, but not directly on, the inferred fitness maxima. Admittedly, this system is optimal for adaptive landscape estimation in some respects: only a few species are involved, they are all (here) sympatric, the important traits are clear, and the phenotypic distribution is nearly continuous. At the same time, however, other aspects of the system are decidedly suboptimal for estimating adaptive landscapes: lifespans are long, only some fitness components can be reliably measured, long-term data are necessary, recapture rates are relatively low, and the populations are "open." Given that other study systems are at least as suitable as ours, even if for different reasons, we anticipate considerable value in applying similar methods to a great diversity of biological communities. Once such data accumulate, perhaps the promise of the theory of adaptive landscapes will finally be realized.

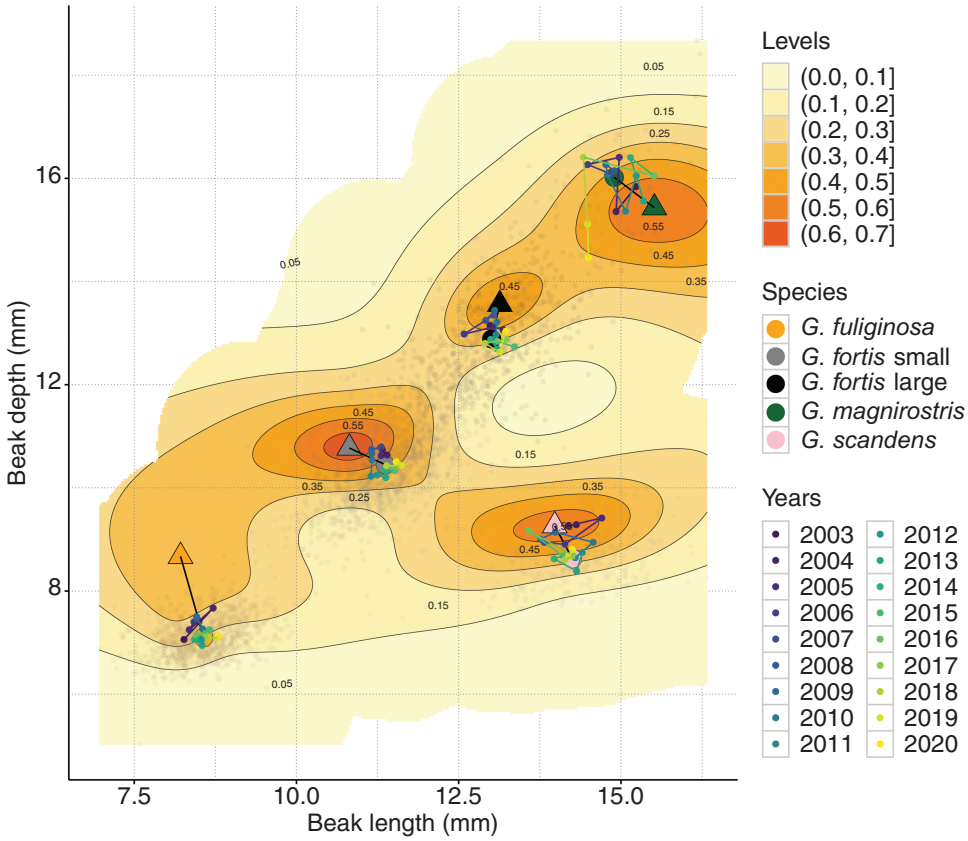

Figure 4. Fitness landscape with black lines connecting the fitness peaks of a species (triangles) to its phenotypic mean (large colored dots). The colored segments (starting from purple to yellow) represent all the phenotypic means in all years (small dots).

Supplementary material

Supplementary material is available online at *Evolution*.

Data availability

The data and scripts are archived on Borealis dataverse at Beausoleil, M.-O., P. L. Carrión, J. Podos, C. Camacho, J. Rabadán-González, R. Richard, K. Lalla, J. A. M. Raeymaekers, S. A. Knutie, L. F. De León, J. A. Chaves, D. H. Clayton, J. A. H. Koop, D. M. T. Sharpe, K. M. Gotanda, S. K. Huber, R. D. H. Barrett, and A. P. Hendry. 2023. Data and code for The fitness landscape of a community of Darwin's finches. Borealis dataverse, https://doi.org/10.5683/SP3/0YIWSE, and on GitHub https://github.com/beausoleilmo/adaptive.landscapes.finches.

Author contributions

M.-O.B. and A.P.H. conceptualized the study, supervised (with R.D.H.B.), wrote the original draft and validated the study. M.-O.B. curated the data, developed the methodology and software for the formal analysis including visualization. M.-O.B., A.P.H., P.L.C., J.P., C.C., J.R.G., R.R., K.L., J.A.M.R., S.A.K., L.F.D.L., S.K.H., J.A.C., D.H.C., J.A.H.K., D.M.T.S., K.M.G., and R.D.H.B. reviewed and edited the manuscript. M.-O.B., P.L.C., J.P., C.C., J.R.G., R.R., K.L., J.A.M.R., S.A.K., L.F.D.L., S.K.H., J.A.C., D.H.C., J.A.H.K., D.M.T.S., K.M.G., and A.P.H. collected the data. M.-O.B., J.P., J.A.M.R., D.H.C., L.F.D.L., J.A.C., D.M.T.S., K.M.G., R.D.H.B., and A.P.H. acquired funding.

Funding

Field work was conducted under the University of Massachusetts Amherst Animal Use Protocols (2003-2006; #23-10-09, 2007-2009; #26-10-16, 2010-2011; #2009-0063, 2012-2013; #2009-0063, 2014-2016; #2013-0087, 2017-2020; #2017-0005) and University of Utah Protocols (2008-2010; #07-08004, 2010-2013; #10-07003) and the Galápagos National Park (Permiso de investigación científica, 2003-2007; #PC-009-98, 2008; #PC-01-08, 2009; #PC-21-07, 2010; #PC-58-10, 2011; #PC-58-10, 2012; #PC-03-12, 2013; #PC-17-13, 2014; #PC-29-14, 2015; #PC-26-15, 2016; #PC-36-16, 2017; #PC-14-17, 2018; #PC-03-18, 2019-2020; #PC-28-19). Field work and equipment were supported by the Natural Sciences and Engineering Research Council of Canada (NSERC) Discovery Grant and a Canada Research Chair to A.P.H. An NSF grant to J.P. covered 2003-2007 field seasons: NSF IBN-0347291. K.M.G. was supported by the University of Cambridge (Clare Hall, Christ's College, and Newnham College), the British Ornithologists Union, a European Society for Evolutionary Biology Godfrey Hewitt Mobility Award, NSERC Vanier and Banting Fellowships, and an FQRNT Postdoctoral Fellowship. Field work was supported by Earthwatch in 2014 and 2015. The research was further supported by an NSERC Discovery Grant and Canada Research Chair to R.D.H.B., and an NSERC Canada Graduate Scholarship, Biodiversity, Ecosystem Services and Sustainability (BESS) NSERC CREATE and Fonds de recherche du Québec, Nature et technologies Scholarship (208545), a National Geographic Young Explorers Grants grant (#WW-170ER-17), and awards given by the Quebec Centre for Biodiversity Science to M.-O.B.

Conflict of interest: The authors declare no conflict of interest. Editorial processing of the manuscript was done independently of L.F.D.L., who is an associate editor of *Evolution*.

Acknowledgments

We thank the Charles Darwin Research Station (CDRS), the Galápagos National Park Service, and the Galápagos Science Center for their valuable logistical support. We thank Dolph Schluter, Trevor Price, and B. Rosemary and Peter R. Grant for providing advice and suggestions on this work. We thank two anonymous reviewers for their thoughtful comments.

References

Arnegard, M. E., McGee, M. D., Matthews, B., Marchinko, K. B., Conte, G. L., Kabir, S., Bedford, N., Bergek, S., Chan, Y. F., Jones, F. C., Kingsley, D. M., Peichel, C. L., & Schluter, D. (2014). Genetics of ecological divergence during speciation. *Nature*, *511*(7509), 307–311. https://doi.org/10.1038/nature13301

Arnold, S. J., Pfrender, M. E., & Jones, A. G. (2001). The adaptive landscape as a conceptual bridge between micro- and macroevolution. *Genetica*, *112-113*(-133), 9–32.

Beausoleil, M. -O., Carrión, P. L., Podos, J., Camacho, C., Rabadán-González, J., Richard, R., Lalla, K., Raeymaekers, J. A. M., Knutie, S. A., De León, L. F., Chaves, J. A., Clayton, D. H., Koop, J. A. H., Sharpe, D. M. T., Gotanda, K. M., Huber, S. K., Barrett, R. D. H., & Hendry, A. P. (2023). Data and code for the fitness landscape of a community of Darwin's finches. Borealis dataverse. https://doi.org/10.5683/SP3/0YIWSE

Beausoleil, M. -O., Frishkoff, L. O., M'Gonigle, L. K., Raeymaekers, J. A. M., Knutie, S. A., De León, L. F., Huber, S. K., Chaves, J. A., Clayton, D. H., Koop, J. A. H., Podos, J., Sharpe, D. M. T., Hendry, A. P., & Barrett, R. D. H. (2019). Temporally varying disruptive selection in the medium ground finch (*Geospiza fortis*). *Proceedings of the Royal Society of London Series B*, *286*(1916), 20192290. https://doi.org/10.1098/rspb.2019.2290

Benaglia, T., Chauveau, D., Hunter, D. R., & Young, D. (2009). mixtools: An R package for analyzing finite mixture models. *Journal of Statistical Software*, *32*(6), 1–29. Version 2.0.0

Benkman, C. W. (1993). Adaptation to single resources and the evolution of Crossbill (*Loxia*) diversity. *Ecological Monographs*, *63*(3), 305–325. https://doi.org/10.2307/2937103

Benkman, C. W. (2003). Divergent selection drives the adaptive radiation of crossbills. *Evolution*, *57*(5), 1176–1181. https://doi.org/10.1111/j.0014-3820.2003.tb00326.x

Boag, P. T. (1983). The heritability of external morphology in Darwin's ground finches (*Geospiza*) on Isla Daphne Major, Galápagos. *Evolution*, *37*(5), 877–894. https://doi.org/10.1111/j.1558-5646.1983.tb05618.x

Boag, P. T., & Grant, P. R. (1984). The classical case of character release: Darwin's finches (*Geospiza*) on Isla Daphne Major, Galápagos. *Biological Journal of the Linnean Society*, *22*, 243–287.

Bolnick, D. I., & Nosil, P. (2007). Natural selection in populations subject to a migration load. *Evolution*, *61*(9), 2229–2243. https://doi.org/10.1111/j.1558-5646.2007.00179.x

Bowman, R. I. (1961). *Morphological differentiation and adaptation in the Galápagos finches*. University of California Publications in Zoology, Berkeley.

Brady, S. P., Bolnick, D. I., Angert, A. L., Gonzalez, A., Barrett, R. D. H., Crispo, E., Derry, A. M., Eckert, C. G., Fraser, D. J., Fussmann, G. F., Guichard, F., Lamy, T., McAdam, A. G., Newman, A. E. M., Paccard, A., Rolshausen, G., Simons, A. M., & Hendry, A. P. (2019a). Causes of maladaptation. *Evolutionary Applications*, *12*(7), 1229–1242. https://doi.org/10.1111/eva.12844

Brady, S. P., Bolnick, D. I., Barrett, R. D. H., Chapman, L., Crispo, E., Derry, A. M., Eckert, C. G., Fraser, D. J., Fussmann, G. F., Gonzalez, A., Guichard, F., Lamy, T., Lane, J., McAdam, A. G., Newman, A. E. M., Paccard, A., Robertson, B., Rolshausen, G., Schulte, P. M., … Hendry, A. P. (2019b). Understanding maladaptation by uniting ecological and evolutionary perspectives. *American Naturalist*, *194*, 495–515.

Carrión, P. L., Raeymaekers, J. A. M., De León, L. F., Chaves, J. A., Sharpe, D. M. T., Huber, S. K., Herrel, A., Vanhooydonck, B., Gotanda, K. M., Koop, J. A. H., Knutie, S. A., Clayton, D. H., Podos, J., & Hendry, A. P. (2022). The terroir of the finch: How spatial and temporal variation shapes phenotypic traits in Darwin's finches. *Ecology and Evolution*, *12*(10), e9399. https://doi.org/10.1002/ece3.9399

Carvajal-Endara, S., Hendry, A. P., Emery, N. C., Neu, C. P., Carmona, D., Gotanda, K. M., Davies, T. J., Chaves, J. A., & Johnson, M. T. J. (2019). The ecology and evolution of seed predation by Darwin's finches on *Tribulus cistoides* on the Galápagos Islands. *Ecological Monographs*, *17*, 73–17.

Chaves, J. A., Cooper, E. A., Hendry, A. P., Podos, J., De León, L. F., Raeymaekers, J. A. M., MacMillan, W. O., & Uy, J. A. C. (2016). Genomic variation at the tips of the adaptive radiation of Darwin's finches. *Molecular Ecology*, *25*, 5282–5295.

Darwin, C. (1859). *On the origin of species by means of natural selection*. Oxford University Press.

De León, L. F., Bermingham, E., Podos, J., & Hendry, A. P. (2010). Divergence with gene flow as facilitated by ecological differences: Within-island variation in Darwin's finches. *Philosophical Transactions of the Royal Society of London Series B*, *365*(1543), 1041–1052. https://doi.org/10.1098/rstb.2009.0314

De León, L. F., Podos, J., Gardezi, T., Herrel, A., & Hendry, A. P. (2014). Darwin's finches and their diet niches: The sympatric coexistence of imperfect generalists. *Journal of Evolutionary Biology*, *27*(6), 1093–1104. https://doi.org/10.1111/jeb.12383

De León, L. F., Raeymaekers, J. A. M., Bermingham, E., Podos, J., Herrel, A., & Hendry, A. P. (2011). Exploring possible human influences on the evolution of Darwin's finches. *Evolution*, *65*, 2258–2272.

De León, L. F., Rolshausen, G., Bermingham, E., Podos, J., & Hendry, A. P. (2012). Individual specialization and the seeds of adaptive radiation in Darwin's finches. *Evolutionary Ecology Research*, *14*, 365–380.

De León, L. F., Sharpe, D. M. T., Gotanda, K. M., Raeymaekers, J. A. M., Chaves, J. A., Hendry, A. P., & Podos, J. (2018). Urbanization erodes niche segregation in Darwin's finches. *Evolutionary Applications*, *12*(7), 1329–1343. https://doi.org/10.1111/eva.12721

DeBruine, L. (2021). faux: Simulation for factorial designs. *Zenodo*. https://doi.org/10.5281/zenodo.7852893. Version 1.2.0.

Estes, S., & Arnold, S. J. (2007). Resolving the paradox of stasis: Models with stabilizing selection explain evolutionary divergence on all timescales. *American Naturalist*, *169*(2), 227–244. https://doi.org/10.1086/510633

Fear, K. K., & Price, T. D. (1998). The adaptive surface in ecology. *Oikos*, *82*, 440–448.

Ford, H. A., Parkin, D. T., & Ewing, A. W. (1973). Divergence and evolution in Darwin's finches. *Biological Journal of the Linnean Society*, *5*(3), 289–295. https://doi.org/10.1111/j.1095-8312.1973.tb00707.x

Foster, D. J., Podos, J., & Hendry, A. P. (2008). A geometric morphometric appraisal of beak shape in Darwin's finches. *Journal of Evolutionary Biology*, *21*(1), 263–275. https://doi.org/10.1111/j.1420-9101.2007.01449.x

Galligan, T. H., Donnellan, S. C., Sulloway, F. J., Fitch, A. J., Bertozzi, T., & Kleindorfer, S. (2012). Panmixia supports divergence with gene flow in Darwin's small ground finch, *Geospiza fuliginosa*, on Santa Cruz, Galápagos Islands. *Molecular Ecology*, *21*(9), 2106–2115. https://doi.org/10.1111/j.1365-294X.2012.05511.x

Garant, D., Forde, S. E., & Hendry, A. P. (2007). The multifarious effects of dispersal and gene flow on contemporary adaptation. *Functional Ecology*, *21*(3), 434–443. https://doi.org/10.1111/j.1365-2435.2006.01228.x

Gavrilets, S. (2004). *Fitness landscapes and the origin of species*. Princeton University Press.

Grant, P. R. (1993). Hybridization of Darwin's finches on Isla Daphne Major, Galápagos. *Philosophical Transaction of the Royal Society of London Series B*, *340*, 127–139.
Grant, P. R. (1999). *Ecology and evolution of Darwin's finches* (2nd ed.). Princeton University Press.
Grant, P. R., & Grant, B. R. (1992). Hybridization of bird species. *Science*, *256*(5054), 193–197. https://doi.org/10.1126/science.256.5054.193
Grant, P. R., & Grant, B. R. (1994). Phenotypic and genetic effects of hybridization in Darwin's finches. *Evolution*, *48*(2), 297–316. https://doi.org/10.1111/j.1558-5646.1994.tb01313.x
Grant, P. R., & Grant, B. R. (1995). The founding of a new population of Darwin's finches. *Evolution*, *49*(2), 229–240. https://doi.org/10.1111/j.1558-5646.1995.tb02235.x
Grant, P. R., & Grant, B. R. (2000). Non-random fitness variation in two populations of Darwin's finches. *Proceedings of the Royal Society of London Series B*, *267*(1439), 131–138. https://doi.org/10.1098/rspb.2000.0977
Grant, P. R., & Grant, B. R. (2002). Unpredictable evolution in a 30-year study of Darwin's finches. *Science*, *296*(5568), 707–711. https://doi.org/10.1126/science.1070315
Grant, P. R., & Grant, B. R. (2011). Causes of lifetime fitness of Darwin's finches in a fluctuating environment. *Proceedings of the National Academy of Sciences of the United States of America*, *108*(2), 674–679. https://doi.org/10.1073/pnas.1018080108
Grant, P. R., & Grant, B. R. (2014). *40 years of evolution*. Princeton University Press.
Grant, P. R., & Grant, B. R. (2019). Hybridization increases population variation during adaptive radiation. *Proceedings of the National Academy of Sciences of the United States of America*, *116*(46), 23216–23224. https://doi.org/10.1073/pnas.1913534116
Grant, P. R., & Grant, B. R. (2021). Morphological ghosts of introgression in Darwin's finch populations. *Proceedings of the National Academy of Sciences of the United States of America*, *118*(31), e2107434118. https://doi.org/10.1073/pnas.2107434118
Hendry, A. P. (2017). *Eco-evolutionary dynamics*. Princeton University Press.
Hendry, A. P., Grant, P. R., Grant, B. R., Ford, H. A., Brewer, M. J., & Podos, J. (2006). Possible human impacts on adaptive radiation: Beak size bimodality in Darwin's finches. *Proceedings of the Royal Society of London Series B*, *273*, 1887–1894.
Hendry, A. P., Huber, S. K., De León, L. F., Herrel, A., & Podos, J. (2009). Disruptive selection in a bimodal population of Darwin's finches. *Proceedings of the Royal Society of London Series B*, *276*(1657), 753–759. https://doi.org/10.1098/rspb.2008.1321
Hendry, A. P., & Taylor, E. B. (2004). How much of the variation in adaptive divergence can be explained by gene flow? An evaluation using lake-stream stickleback pairs. *Evolution*, *58*(10), 2319–2331. https://doi.org/10.1111/j.0014-3820.2004.tb01606.x
Holzman, R., Keren, T., Kiflawi, M., Martin, C. H., China, V., Mann, O., & Olsson, K. H. (2022). A new theoretical performance landscape for suction feeding reveals adaptive kinematics in a natural population of reef damselfish. *Journal of Experimental Biology*, *225*(13), jeb243273. https://doi.org/10.1242/jeb.243273
Huber, S. K., De León, L. F., Hendry, A. P., Bermingham, E., & Podos, J. (2007). Reproductive isolation of sympatric morphs in a population of Darwin's finches. *Proceedings of the Royal Society of London Series B*, *274*(1619), 1709–1714. https://doi.org/10.1098/rspb.2007.0224
Kaplan, J. (2008). The end of the adaptive landscape metaphor? *Biology and Philosophy*, *23*(5), 625–638. https://doi.org/10.1007/s10539-008-9116-z
Kleindorfer, S., Chapman, T. W., Winkler, H., & Sulloway, F. J. (2006). Adaptive divergence in contiguous populations of Darwin's Small Ground Finch (*Geospiza fuliginosa*). *Biological Journal of the Linnean Society*, *110*, 45–59.
Kruuk, L. E. B. (2004). Estimating genetic parameters in natural populations using the "animal model". *Philosophical Transaction of the Royal Society of London Series B*, *359*(1446), 873–890. https://doi.org/10.1098/rstb.2003.1437
Lack, D. L. (1947). *Darwin's finches*. Cambridge University Press.
Lamichhaney, S., Berglund, J., Almén, M. S., Maqbool, K., Grabherr, M., Martinez-Barrio, A., Promerová, M., Rubin, C. -J., Wang, C., Zamani, N., Grant, B. R., Grant, P. R., Webster, M. T., & Andersson, L. (2015). Evolution of Darwin's finches and their beaks revealed by genome sequencing. *Nature*, *518*(7539), 371–375. https://doi.org/10.1038/nature14181
Lamichhaney, S., Han, F., Berglund, J., Wang, C., Almén, M. S., Webster, M. T., Grant, B. R., Grant, P. R., & Andersson, L. (2016). A beak size locus in Darwin's finches facilitated character displacement during a drought. *Science*, *352*(6284), 470–474. https://doi.org/10.1126/science.aad8786
Lande, R. (1976). Natural selection and random genetic drift in phenotypic evolution. *Evolution*, *30*(2), 314–334. https://doi.org/10.1111/j.1558-5646.1976.tb00911.x
Lande, R. (1979). Quantitative genetic analysis of multivariate evolution, applied to brain: body size allometry. *Evolution*, *33*(1Part2), 402–416. https://doi.org/10.1111/j.1558-5646.1979.tb04694.x
Martin, C. H., & Gould, K. J. (2020). Surprising spatiotemporal stability of a multi-peak fitness landscape revealed by independent field experiments measuring hybrid fitness. *Evolution Letters*, *4*(6), 530–544. https://doi.org/10.1002/evl3.195
Martin, C. H., & Wainwright, P. C. (2013). Multiple fitness peaks on the adaptive landscape drive adaptive radiation in the wild. *Science*, *339*(6116), 208–211. https://doi.org/10.1126/science.1227710
McGhee, G. R., Jr. (2006). *The geometry of evolution: Adaptive landscapes and theoretical morphospaces*. Cambridge University Press.
Merrell, D. J. (1994). *The adaptive seascape: The mechanism of evolution*. University of Minnesota Press.
Nagy, E. S. (1997). Selection for native characters in hybrids between two locally adapted plant subspecies. *Evolution*, *51*(5), 1469–1480. https://doi.org/10.1111/j.1558-5646.1997.tb01470.x
Nagy, E. S., & Rice, K. J. (1997). Local adaptation in two subspecies of an annual plant: Implications for migration and gene flow. *Evolution*, *51*(4), 1079–1089. https://doi.org/10.1111/j.1558-5646.1997.tb03955.x
Nosil, P. (2012). *Ecological speciation*. Oxford University Press.
Oksanen, J., Simpson, G. L., Blanchet, F. G., Kindt, R., Legendre, P., Minchin, P. R., O'Hara, R. B., Sólymos, P., McGlinn, D., Stevens, M. H. H., Szöecs, E., Wagner, H., Barbour, M., Bedward, M., Bolker, B., Borcard, D., Carvalho, G., Chirico, M., De Cáceres, M., … Weedon, J. (2022). vegan: Community ecology package. Version 2.6-4.
Patton, A. H., Richards, E. J., Gould, K. J., Buie, L. K., & Martin, C. H. (2022). Hybridization alters the shape of the genotypic fitness landscape, increasing access to novel fitness peaks during adaptive radiation. *eLife*, *11*, e72905. https://doi.org/10.7554/eLife.72905
Petren, K., Grant, P. R., Grant, B. R., & Keller, L. F. (2005). Comparative landscape genetics and the adaptive radiation of Darwin's finches: The role of peripheral isolation. *Molecular Ecology*, *14*(10), 2943–2957. https://doi.org/10.1111/j.1365-294X.2005.02632.x
Pfaender, J., Hadiaty, R. K., Schliewen, U. K., & Herder, F. (2016). Rugged adaptive landscapes shape a complex, sympatric radiation. *Proceedings of the Royal Society of London Series B*, *283*(1822), 20152342. https://doi.org/10.1098/rspb.2015.2342
Pigliucci, M. (2008). Sewall Wright's adaptive landscapes: 1932 vs. 1988. *Biology and Philosophy*, *23*(5), 591–603. https://doi.org/10.1007/s10539-008-9124-z
Podos, J. (2010). Acoustic discrimination of sympatric morphs in Darwin's finches: A behavioural mechanism for assortative mating? *Philosophical Transaction of the Royal Society of London Series B*, *365*(1543), 1031–1039. https://doi.org/10.1098/rstb.2009.0289
Price, T. D., Grant, P. R., Gibbs, H. L., & Boag, P. T. (1984). Recurrent patterns of natural selection in a population of Darwin's finches. *Nature*, *309*(5971), 787–789. https://doi.org/10.1038/309787a0
R Core Team. (2023). *R: A language and environment for statistical computing*. R Foundation for Statistical Computing.
Ratcliffe, L. M., & Grant, P. R. (1983). Species recognition in Darwin's finches (*Geospiza*, Gould). I. Discrimination by morphological cues. *Animal Behaviour*, *31*, 1139–1153.

Raup, D. M. (1967). Geometric analysis of shell coiling: coiling in Ammonoids. *Journal of Paleolimnology*, *41*, 43–65.

Schemske, D. W., & Bradshaw, H. D. (1999). Pollinator preference and the evolution of floral traits in monkeyflowers (*Mimulus*). *Proceedings of the National Academy of Sciences of the United States of America*, *96*(21), 11910–11915. https://doi.org/10.1073/pnas.96.21.11910

Schluter, D. (1984). Morphological and phylogenetic relations among the Darwin's finches. *Evolution*, *38*(5), 921–930. https://doi.org/10.1111/j.1558-5646.1984.tb00363.x

Schluter, D. (2000). *The ecology of adaptive radiation*. Oxford University Press.

Schluter, D., & Grant, P. R. (1984). Determinants of morphological patterns in communities of Darwin's finches. *American Naturalist*, *123*(2), 175–196. https://doi.org/10.1086/284196

Schluter, D., & Nychka, D. (1994). Exploring fitness surfaces. *American Naturalist*, *143*(4), 597–616. https://doi.org/10.1086/285622

Siepielski, A. M., Dibattista, J. D., & Carlson, S. M. (2009). It's about time: The temporal dynamics of phenotypic selection in the wild. *Ecology Letters*, *12*(11), 1261–1276. https://doi.org/10.1111/j.1461-0248.2009.01381.x

Siepielski, A. M., Morrissey, M. B., Buoro, M., Carlson, S. M., Caruso, C. M., Clegg, S. M., Coulson, T., DiBattista, J., Gotanda, K. M., Francis, C. D., Hereford, J., Kingsolver, J. G., Augustine, K. E., Kruuk, L. E. B., Martin, R. A., Sheldon, B. C., Sletvold, N., Svensson, E. I., Wade, M. J., & MacColl, A. D. C. (2017). Precipitation drives global variation in natural selection. *Science*, *355*, 959–962.

Simpson, G. G. (1944). *Tempo and mode in evolution*. Columbia University Press.

Sinervo, B., Zamudio, K., Doughty, P., & Huey, R. B. (1992). Allometric engineering: A causal analysis of natural selection on offspring size. *Science*, *258*(5090), 1927–1930. https://doi.org/10.1126/science.258.5090.1927

Smith, T. B. (1990). Natural selection on bill characters in the two bill morphs of the African finch *Pyrenestes ostrinus*. *Evolution*, *44*(4), 832–842. https://doi.org/10.1111/j.1558-5646.1990.tb03808.x

Smith, T. B. (1993). Disruptive selection and the genetic basis of bill size polymorphism in the African finch *Pyrenestes*. *Nature*, *363*(6430), 618–620. https://doi.org/10.1038/363618a0

Smith, T. B., & Girman, D. J. (2000). Reaching new adaptive peaks: Evolution of alternative bill forms in an African finch. In T. A. Mousseau, B. Sinervo, & J. A. Endler (Eds.), *Adaptive genetic variation in the wild* (pp. 139–156). Oxford University Press.

Stayton, C. T. (2019). Performance in three shell functions predicts the phenotypic distribution of hard-shelled turtles. *Evolution*, *73*(4), 720–734. https://doi.org/10.1111/evo.13709

Stoffel, M. A., Nakagawa, S., & Schielzeth, H. (2017). rptR: Repeatability estimation and variance decomposition by generalized linear mixed-effects models. *Methods in Ecology and Evolution*, *8*(11), 1639–1644. Version 0.9.22. https://doi.org/10.1111/2041-210x.12797

Svensson, E. I., & Calsbeek, R. (2012a). *The adaptive landscape in evolutionary biology*. Oxford University Press.

Svensson, E. I., & Calsbeek, R. (2012b). The past, the present, and the future of the adaptive landscape. In E. Svensson, & R. Calsbeek (Eds.), *The adaptive landscape in evolutionary biology* (pp. 1–10). Oxford University Press.

Tseng, Z. J. (2013). Testing adaptive hypotheses of convergence with functional landscapes: A case study of bone-cracking hypercarnivores. *PLoS One*, *8*(5), e65305. https://doi.org/10.1371/journal.pone.0065305

Wilson, A. J., Réale, D., Clements, M. N., Morrissey, M. M., Postma, E., Walling, C. A., Kruuk, L. E. B., & Nussey, D. H. (2010). An ecologist's guide to the animal model. *Journal of Animal Ecology*, *79*(1), 13–26. https://doi.org/10.1111/j.1365-2656.2009.01639.x

Wood, S. N. (2003). Thin plate regression splines. *Journal of the Royal Statistical Society: Series B*, *65*(1), 95–114. https://doi.org/10.1111/1467-9868.00374

Wood, S. N., Pya, N., & Säfken, B. (2016). Smoothing parameter and model selection for general smooth models. *Journal of the American Statistical Association*, *111*(516), 1548–1563. https://doi.org/10.1080/01621459.2016.1180986

Wood, S. N., Scheipl, F., & Faraway, J. J. (2013). Straightforward intermediate rank tensor product smoothing in mixed models. *Statistics and Computing*, *23*(3), 341–360. https://doi.org/10.1007/s11222-012-9314-z

Wright, S. (1932). The roles of mutation, inbreeding, crossbreeding and selection in evolution. *Proceedings of the Sixth International Congress of Genetics*, *1*, 356–366.